J Appl Electrochem (2008) 38:289–295
DOI 10.1007/s10800-007-9437-7

ORIGINAL PAPER

Some new triazole derivatives as inhibitors for mild steel corrosion in acidic medium

Wei-hua Li · Qiao He · Sheng-tao Zhang · Chang-ling Pei · Bao-rong Hou

Received: 11 May 2007 / Revised: 5 October 2007 / Accepted: 17 October 2007 / Published online: 1 November 2007

Abstract Two triazole derivatives, 3,4-dichloro-acetophenone-*O*-1′-(1′,3′,4′-triazolyl)-methaneoxime (4-DTM) and 2,5-dichloro-acetophenone-*O*-1′-(1′,3′,4′-triazolyl)-methaneoxime (5-DTM) were synthesized, and the inhibition effects for mild steel in 1 M HCl solutions were investigated by weight loss measurements, electrochemical tests and scanning electronic microscopy (SEM). The weight loss measurements showed that these compounds have excellent inhibiting effect at a concentration of 1.0×10^{-3} M. The potentiodynamic polarization experiment revealed that the triazole derivatives are inhibitors of mixed-type and electrochemical impedance spectroscopy (EIS) confirmed that changes in the impedance parameters (R_{ct} and C_{dl}) are due to surface adsorption. The inhibition efficiencies obtained from weight loss measurements and electrochemical tests were in good agreement. Adsorption followed the Langmuir isotherm with negative values of the free energy of adsorption ΔG^{o}_{ads}. The thermodynamic parameters of adsorption were determined and are discussed. Results show that both 4-DTM and 5-DTM are good inhibitors for mild steel in acid media.

W.-h. Li (✉) · B.-r. Hou
Institute of Oceanology, Chinese Academy of Sciences, Qingdao 266071, China
e-mail: google7723@163.com

Q. He · S.-t. Zhang
College of Chemistry and Chemical Engineering, Chongqing University, Chongqing 400044, China

C.-l. Pei
School of Civil Engineering, Qingdao Technological University, Qingdao 266033, China

Keywords Triazole derivative · Acid inhibitor · Potentiodynamic polarization · EIS · Langmuir adsorption isotherm

1 Introduction

Acid solutions are widely used in industry, some of the important fields of application being acid pickling of iron and steel, chemical cleaning and processing, ore production and oil well acidification. The use of inhibitors is one of the most economical and practical methods of reducing corrosive attack on metals [1–3]. During the past decade, the inhibition of mild steel corrosion in acid solutions by various types of organic inhibitors has attracted much attention [4–6]. It is generally accepted that inhibitors act via their functional groups adsorbing on the metal surface, changing the corrosion resistance properties of the metal [7, 8]. Recently it has been shown that the adsorption of organic inhibitors mainly depends on physicochemical and electronic properties of the molecule, related to their functional groups, steric effects, electron density of donor atoms, and the π orbital character of donating electrons [9, 10].

Most of the well-known organic inhibitors contain nitrogen, sulphur, oxygen, phosphorous and aromatic rings or multiple bonds in their molecular structure [11, 12]. Examples are triazole-type compounds, containing several heterocyclic structures, which have excellent inhibition properties for the corrosion of many metals in various aggressive media [13, 14]. However, the disadvantages of some organic inhibitors are their toxicity. In view of environmental protection requirements, the use of these organic inhibitors is nowadays quite limited. Therefore, investigating new environmentally friendly inhibitors for steel corrosion in acid media is important.

Two triazole derivatives, 3,4-dichloro-acetophenone-*O*-1′-(1′,3′,4′-triazolyl)-methaneoxime (4-DTM) and 2,5-dichloro-acetophenone-*O*-1′-(1′,3′,4′-triazolyl)-methaneoxime (5-DTM), respectively, were synthesized in our laboratory, and purified and characterized by IR, ^{1}HNMR, MS. The synthetic route and molecular structures are shown in Fig. 1.

The objective of the present work was to study the inhibition effect of the newly synthesized non-toxic triazole derivatives on the corrosion of mild steel in hydrochloric acid solutions. The inhibition performance was evaluated by weight loss, potentiodynamic polarization, electrochemical impedance spectroscopy (EIS), and scanning electronic microscopy (SEM).

2 Experimental

2.1 Solutions and specimens preparation

Solutions of 1 M HCl were prepared by dilution of analytical grade 37% HCl with bidistilled water. The concentration range of the inhibitors used was 1×10^{-5}M–1×10^{-3} M, and blank solution was used for comparison. Corrosion experiments were performed on mild steel of the following percentage composition (wt%): 0.17 °C, 0.46 Mn; 0.26 Si; 0.017 S; 0.019 Cu, and the remainder Fe.

2.2 Weight loss measurements

Prior to measurements, the steel specimens were mechanically cut into pieces of dimensions $30 \times 15 \times 15$ mm and polished with emery paper up to 1200 grade. These were immersed in 1 M HCl solutions with and without different concentrations of inhibitors for 3 h at 298 K. Then the specimens were removed, rinsed in water and acetone and finally dried in a desiccator. The loss in weight was determined by analytical balance.

2.3 Electrochemical experiments

The mild steel specimens used as working electrodes were embedded in epoxy resin, leaving an exposed surface area of 1 cm^2 to the electrolyte. A saturated calomel electrode (SCE) and a platinum electrode were used, respectively, as reference and auxiliary electrodes. All potentials are given on the SCE scale. The electrochemical experiments were carried out with a PARSTAT 2273 Potentiostat/Galvanostat in non-deaerated solutions at 298 ± 2 K.

The working electrode was immersed in 1 M HCl solution for approximate 30 min until a steady-state open-circuit potential (OCP) was obtained. The potentiodynamic polarization curves were recorded from −200 to +200 mV_{SCE} (versus OCP) with a scan rate of 0.5 mV s^{-1} and the data were collected and analyzed by electrochemical software PowerSuite ver.2.58. EIS measurements were carried out at steady state OCP with amplitude of 10 mV ac sine wave. The frequency range was 100 kHz–10 mHz. The impedance data were analyzed and fitted using ZSimpWin ver.3.21.

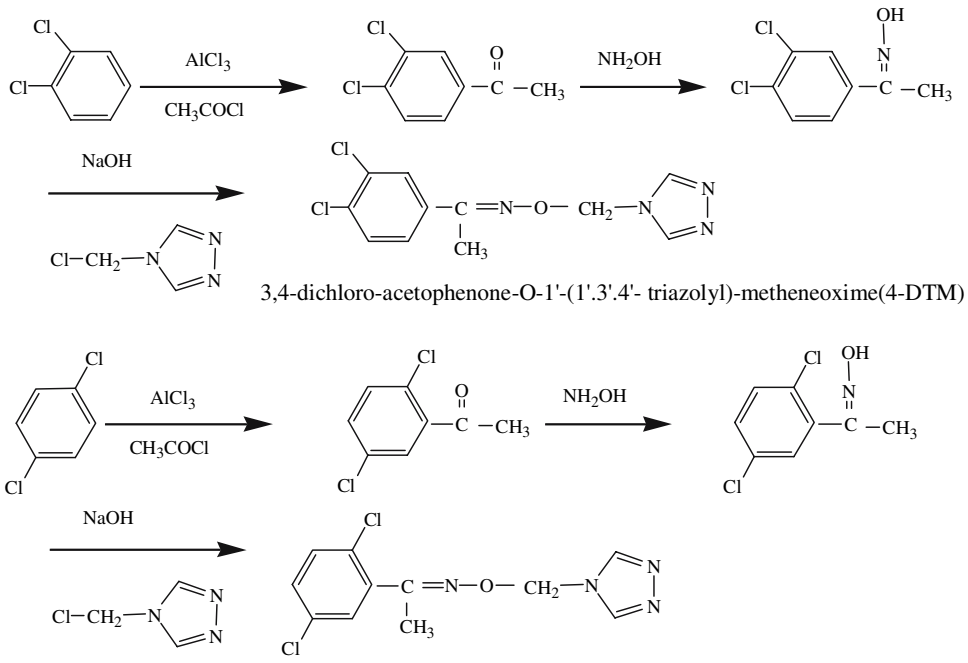

Fig. 1 The synthetic route and molecular structures of 4-DTM and 5-DTM

3 Results and discussion

3.1 SEM analyses

The SEM photographs are given in Fig. 2. The surface morphology of the sample before immersion in 1 M HCl solutions show a freshly polished steel surface (Fig. 4a), and the scratches are from the mechanical polishing treatment. Figure 2b shows the surface morphology in the absence of the inhibitor, the mild steel surface was highly corroded with areas of localized corrosion. SEM images of the mild steel surface after immersion in 1 M HCl with 1.0×10^{-3} M inhibitor of 4-DTM and 5-DTM are shown in Fig. 2c and d where it can be seen that the rate of corrosion is suppressed, and there is little acid corrosion product on the steel surface, even the original polishing scratches are seen. This clearly reveals that there is a good protective film on the mild steel surface, decreasing the extent of corrosion.

3.2 Electrochemical experiments

3.2.1 Potentiodynamic polarization curves

Polarization curves for mild steel in 1 M HCl solutions without and with addition of different concentrations of 4-DTM and 5-DTM are shown in Fig. 3a and b. The anodic and cathodic current-potential curves are extrapolated up to their intersection at the point where corrosion current density (I_{corr}) and corrosion potential (E_{corr}) are obtained. The electrochemical parameters E_{corr}, I_{corr}, anodic and cathodic Tafel slopes (β_a, β_c) obtained from polarization measurements are listed in Table 1. The inhibition efficiency was calculated from expression [15] (1):

$$\mathrm{IE}\% = \frac{i^{o}_{corr} - i_{corr}}{i^{o}_{corr}} \times 100 \quad (1)$$

where i_{corr} and i^{o}_{corr} are the corrosion current with and without inhibitor.

From Fig. 3a and b it can be seen that the cathodic Tafel slopes (β_c) remain almost constant with increasing inhibitor concentration. This indicates that hydrogen evolution is activation-controlled, and the addition of inhibitors does not change the mechanism of the cathodic hydrogen evolution reaction [16, 17].

For the anodic polarization curves of 4-DTM, at concentrations of 1.0×10^{-3} M or higher and for potentials higher than -300 mV_{SCE}, the corrosion current increases more clearly with rising potential and the same result is observed in the anodic polarization curves for 5-DTM. The phenomenon of significant dissolution is due to the desorption rate of the inhibitor being higher than its adsorption rate [18]. This result shows that the inhibition effect of these compounds depends on the electrode potential.

The inhibition efficiency increases with increasing inhibitor concentration and reaches its highest value at a

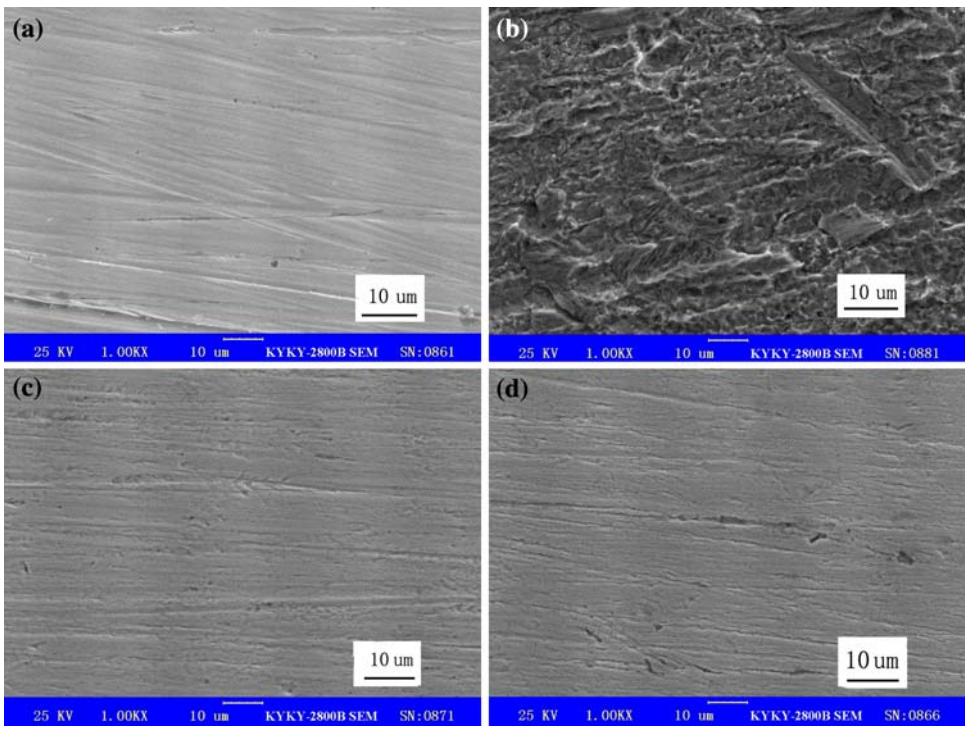

Fig. 2 SEM micrographs of mild steel samples (**a**) only surface polishing, (**b**) after immersion in 1 M HCl without inhibitor, (**c**) after immersion in 1 M HCl in presence of 1.0×10^{-3} M 4-DTM, (**d**) after immersion in 1 M HCl in presence of 1.0×10^{-3} M 5-DTM

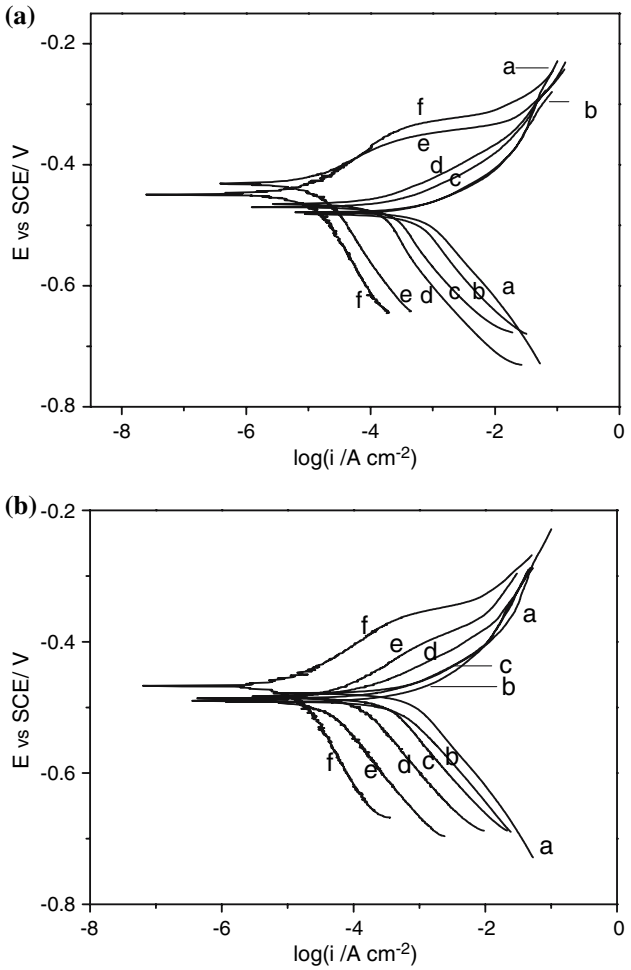

Fig. 3 Potentiodynamic polarization curves for mild steel in 1 M HCl with different concentrations: (**a**) 4-DTM: a, Blank; b, 1.0×10^{-5} M; c, 3.2×10^{-5} M; d, 1.0×10^{-4} M; e, 3.2×10^{-4} M; f, 1.0×10^{-3} M; (**b**) 5-DTM: a, Blank; b, 1.0×10^{-5} M; c, 3.2×10^{-5} M; d, 1.0×10^{-4} M; e, 3.2×10^{-4} M; f, 1.0×10^{-3} M

concentration of 1.0×10^{-3} M, it exhibits both anodic and cathodic inhibition performance via adsorption on the steel surface blocking active sites [19]. According to Riggs and others [20], if the displacement in E_{corr} is >85 mV with respect to E^{o}_{corr}, the inhibitor can be seen as a cathodic or anodic type. In our study the maximum displacement was 40 mV, which indicates that the inhibitors are mixed-type.

3.2.2 *Electrochemical impedance spectroscopy (EIS)*

The Nyquist plots are shown in Fig. 4a and b, where it can be seen that the impedance spectra are similar, exhibiting a single semicircle at high frequency. The high frequency capacitive loop is attributable to charge transfer of the corrosion process, and the diameter of the semicircle increases with increasing inhibitor concentration. As is clear from Fig. 4, the impedance spectra do not present perfect semicircles. The "depressed" semicircles have a center under the real axis, and can be seen as depressed capacitive loops. Such phenomena often correspond to surface heterogeneity which may be the result of surface roughness, dislocations, distribution of the active sites or adsorption of inhibitors [21, 22]. In order to fit and analyze the EIS data, an equivalent circuit was selected and is shown in Fig. 5. This circuit is generally used to describe the iron/acid interface model [23]. In this equivalent circuit, R_S is the electrolyte resistance, Rct is the charge transfer resistance and CPE is a constant phase element. The impedance function of the CPE is as follows:

$$Z_{CPE} = Y^{-1}(j\omega)^{-n} \quad (2)$$

where Y is a proportional factor, ω is the angular frequency, and the deviation parameter n is a valuable

Table 1 Potentiodynamic polarization parameters for mild steel in 1 M HCl with different concentrations of 4-DTM and 5-DTM

Concentration (M)	E_{corr} (vs. SCE) (mV)	I_{corr} (μA cm^{-2})	β_c (mV dec^{-1})	β_a (mV dec^{-1})	IE (%)
Blank	−479.1	868	134.6	69.0	
4-DTM					
1×10^{-5}	−481.0	629	140.1	64.9	27.5
3.2×10^{-5}	−470.1	234	144.1	51.4	73.0
1.0×10^{-4}	−465.2	123	140.0	49.1	85.8
3.2×10^{-4}	−430.8	14	149.6	58.5	98.4
1.0×10^{-3}	−448.7	11	158.5	80.4	98.7
5-DTM					
1×10^{-5}	−492.1	664	135.8	71.4	23.5
3.2×10^{-5}	−488.5	418	133.7	64.5	51.8
1.0×10^{-4}	−486.0	127	123.9	55.8	85.3
3.2×10^{-4}	−489.8	42	134.4	60.8	95.1
1.0×10^{-3}	−466.7	14	137.3	68.2	98.4

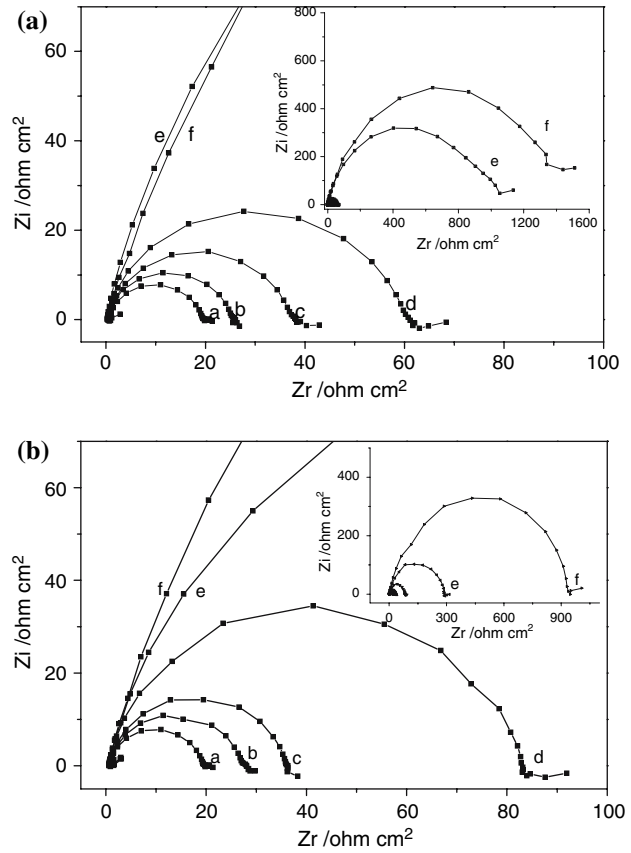

Fig. 4 Nyquist diagrams for mild steel in 1 M HCl containing different concentrations of (**a**) 4-DTM: a, Blank; b, 1.0×10^{-5} M; c, 3.2×10^{-5} M; d, 1.0×10^{-4} M; e, 3.2×10^{-4} M; f, 1.0×10^{-3} M; (**b**) 5-DTM: a, Blank; b, 1.0×10^{-5} M; c, 3.2×10^{-5} M; d, 1.0×10^{-4} M; e, 3.2×10^{-4} M; f, 1.0×10^{-3} M

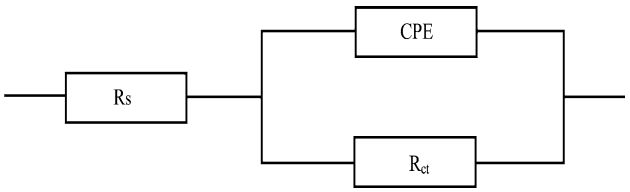

Fig. 5 The equivalent circuit model used to fit the EIS experiment data for mild steel in 1 M HCl solutions

criterion of the nature of the metal surface and reflects microscopic fluctuations of the surface. For $n = 0$, Z_{CPE} represents a resistance with $R = Y^{-1}$; $n = -1$ an inductance with $L = Y^{-1}$, $n = 1$ a ideal capacitor with $C = Y$ [24]. In real iron/acid interface systems, ideal capacitive behavior is not observed due to roughness, or uneven current distributions on the electrode surface; therefore a CPE is used instead of a capacitor C_{dl} (double layer capacity) to fit more accurately the impedance behavior of the electrical double layer. The capacitance values can be described by CPE parameter values Y and n using the expression [25]

$$C_{id} = \frac{Y\omega^{n-1}}{\sin(n\frac{\pi}{2})} \tag{3}$$

According to the equivalent circuit, the impedance data were fitted and the electrochemical parameters R_{ct} and C_{dl} are listed in Table 2. The inhibition efficiency, IE%, in different concentrations of 4-DTM and 5-DTM were calculated from the charge transfer resistance according to equation:

$$\text{IE\%} = \frac{R_{ct} - R_{ct}^{o}}{R_{ct}} \times 100 \tag{4}$$

where R_{ct} and R_{ct}^{o} represent the charge transfer resistance in the absence and presence of inhibitor. The values of *Rct* increase with increasing inhibitor concentration and the results indicate that charge transfer process mainly controls the corrosion process. The decrease in C_{dl} is due to adsorption which displaces water molecules originally adsorbed on the mild steel surface and decreases the active surface area. The values of double-layer capacitance decrease with increasing inhibitor concentration indicating that 4-DTM and 5-DTM molecules function by adsorption at the metal/solution interface, leading to a protective film on the steel surface [26]. In addition, the deviation parameter n has a tendency to decrease with increasing inhibitor concentration. The decrease in n may be connected with surface roughening which, due to the inhibitor molecules adsorbed on the metal surface, increase the heterogeneity [27]. The inhibiting efficiencies calculated by EIS and potentiodynamic polarization are in reasonably good agreement.

3.3 Weight loss measurements

Values of inhibition efficiency IE% and corrosion rate (mg cm^{-2} h^{-1}) obtained from the weight loss method for various concentrations of 4-DTM and 5-DTM at 298 K are summarized in Table 3. The inhibition efficiency IE% was calculated from Eq. 5:

$$\text{IE} = \frac{W^{o} - W}{W^{o}} \times 100 \tag{5}$$

where W^{o} and W are the corrosion rates in the absence and presence of the inhibitor, respectively. It can be seen in Table 3 that increase in inhibitor concentration leads to a decrease in corrosion rate and an increase in inhibition efficiency. At the highest concentration of 1×10^{-3} M, the inhibition efficiency attains about 92% for 4-DTM, and 94% for 5-DTM, indicating that both triazoles are excellent inhibitors. Also the inhibition efficiencies obtained from electrochemical measurements are not the same as those

Table 2 Impedance data of mild steel in 1 M HCl in absence and presence of different concentrations of 4-DTM and 5-DTM

Concentration (M)	R_s (Ω cm^2)	R_{ct} (Ω cm^2)	C_{dl} (μF cm^{-2})	n	IE (%)
Blank	0.71	19.02	173	0.913	
4-DTM					
1×10^{-5}	0.45	24.8	152	0.969	23.3
3.2×10^{-5}	0.53	37.48	112	0.969	49.5
1.0×10^{-4}	0.56	61	102	0.929	68.8
3.2×10^{-4}	0.51	1014	38	0.866	98.1
1.0×10^{-3}	1.69	1474	50	0.807	98.7
5-DTM					
1×10^{-5}	1.85	25.6	125	0.967	25.8
3.2×10^{-5}	1.80	33.9	106	0.968	43.9
1.0×10^{-4}	1.21	82.3	71	0.925	76.9
3.2×10^{-4}	1.46	285.9	47	0.869	93.3
1.0×10^{-3}	1.83	948.7	42	0.829	98.0

from weight loss measurements. The difference can be attributed to the fact that the weight loss method gives average corrosion rates, whereas the electrochemical method gives instantaneous rates.

3.4 Adsorption isotherm

It is widely acknowledged that basic information on the interaction between an inhibitor and the mild steel surface is provided by the adsorption isotherm. The surface coverage (θ) of different concentrations of inhibitor in acidic medium can be calculated by weight loss measurement, the equation being as follows [28]:

Table 3 Values of inhibition efficiency of mild steel in 1 M HCl in absence and presence of different concentrations of 4-DTM and 5-DTM at 298 K

Concentration (M)	Weight loss (mg cm^{-2} h^{-1})	IE (%)
Blank	6.205	
4-DTM		
1×10^{-5}	5.872	5.34
3.2×10^{-5}	4.060	34.6
1.0×10^{-4}	2.224	64.2
3.2×10^{-4}	0.448	91.9
1.0×10^{-3}	0.498	92.8
5-DTM		
1×10^{-5}	5.667	8.7
3.2×10^{-5}	3.735	39.8
1.0×10^{-4}	1.324	78.7
3.2×10^{-4}	0.547	91.2
1.0×10^{-3}	0.376	94.0

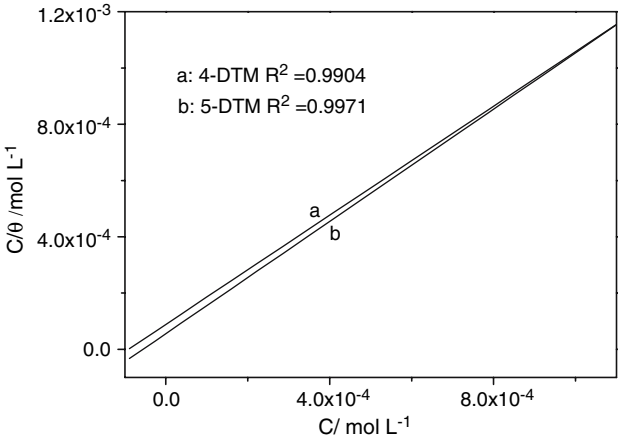

Fig. 6 Langmuir isotherm adsorption of 4-DTM and 5-DTM on mild steel in 1 M HCl at 298 K

$$\theta = \frac{W_0 - W}{W_0} \tag{6}$$

The values of θ can be used to determine the thermodynamic parameters and the mode of the adsorption process. The adsorption models considered were:

Temkin isotherm $\exp(f\,\theta) = k_{ads}\,C$
Langmuir isotherm $\theta/(1-\theta) = k_{ads}\,C$
Frumkin isotherm $\theta/(1-\theta)\exp(-2f\,\theta) = k_{ads}\,C$
Freundluich isotherm $\theta = k_{ads}\,C$

where k_{ads} is the equilibrium constant of the inhibitor adsorption process, C is the inhibitor concentration and f is the parameter related to the variation in adsorption energy with surface coverage. The Langmuir isotherm was found to provide the best description of the adsorption behavior. Plots of C/θ versus C yield a straight line as shown in Fig. 6. In both cases the linear regression coefficients (R^2) are almost equal to 1 and the slopes are very close to 1, indicating that the adsorption of 4-DTM and 5-DTM obeys the Langmuir isotherm and there is negligible interaction between the adsorbed molecules.

k_{ads} values can be calculated from the intercepts of the straight lines on the C/θ-axis, and the constant of adsorption, k_{ads} is related to the standard free energy of adsorption, ΔG^o_{ads}, with the following equation [29]:

$$k_{ads} = (1/55.5)\exp(-\Delta G^o_{ads}/RT) \tag{7}$$

the value 55.5 is the molar concentration of water in solution in mol L^{-1} [30]. The thermodynamic parameters for adsorption obtained from the Langmuir isotherm are listed in Table 4.

The negative values of ΔG^o_{ads} suggest that the adsorption of 4-DTM and 5-DTM onto the steel surface is a spontaneous process and the adsorbed layer is stable. Generally,

Table 4 Thermodynamic parameters for the adsorption of 4-DTM and 5-DTM in 1 M HCl on the mild steel at 298 K

	k_{ads} (M^{-1})	ΔG^o_{ads} (kJ mol^{-1})
4-DTM	1.12×10^4	−33.07
5-DTM	1.79×10^4	−34.23

for values of ΔG^o_{ads} up to -20 kJ mol^{-1}, the type of adsorption is regarded as physisorption. The adsorption process is due to electrostatic interactions between the charged molecules and the charged metal [28, 31]. Values around -40 kJ mol^{-1} or higher are associated with chemisorption [32]. The calculated ΔG^o_{ads} values are -33.07 and -34.23 kJ mol^{-1} indicated that adsorption may involve complex interactions: chemical adsorption and physical adsorption. The possible adsorption mechanisms is: (a) Direct adsorption on the basis of donor–acceptor interactions between the lone pairs of electrons of chloride atoms, π-electrons of –C=N, phenyl, triazolyl groups and the vacant *d*-orbitals of iron surface atoms. This process is called chemical adsorption. (b) Protonation of the 4-DTM and 5-DTM molecule in acid solution, forming cations, the adsorption process can occur via electrostatic interaction between the positively charged heterocyclic nitrogen atoms and the negatively charged mild steel surface. This process is called physical adsorption. (c) Indirect adsorption of the protonated triazoles on the mild steel surface through a synergistic effect with chloride ions from hydrochloric acid solution.

4 Conclusion

1. All measurements showed that the triazole derivatives have excellent inhibition properties for the corrosion of mild steel in 1 M HCl solutions. The inhibition efficiency increases with inhibitor concentration and reaches its highest value at 1.0×10^{-3} M.
2. Potentiodynamic polarization measurements show that the triazole derivatives act as mixed-type inhibitors. EIS measurements also indicate that the inhibitors increase the charge transfer resistances and show that the inhibitive performance depends on adsorption of the molecules on the metal surface.
3. The inhibiting efficiencies determined by potentiodynamic polarization, EIS, and weight loss methods are in reasonably good agreement.
4. The adsorption model obeys the Langmuir isotherm at 298 K. The negative values of ΔG^o_{ads} indicate that the adsorption of the triazole molecule is a spontaneous process, and three different adsorption mechanisms may take place on the mild steel surface.

Acknowledgements The authors gratefully acknowledge the support of K.C. Wang Education Foundation, Hong Kong and the Knowledge Innovation Project of The Chinese Academy of Science (Grant No. KZXCX2-YW-210).

References

1. Khaled KF, Hackerman N (2003) Electrochim Acta 48:2715
2. Ali SA, Saeed MT, Rahman SV (2003) Corros Sci 45:253
3. Sastri VS, Perumareddi JR (1997) Corrosion 53:617
4. Bentiss F, Lagrene M, Traisnel M, Mernari B, Elattari H (1999) J Appl Electrochem 29:1073
5. Quraishi MA, Jamal D (2000) Corrosion 56:156
6. Moretti G, Guidi F, Grion G (2004) Corros Sci 46:387
7. Bouklah M, Ouassini A, Hammouti B, El-Idrissi A (2005) Appl Surf Sci 250:50
8. Migahed MA, Mohamed HM, Al-Sabagh AM (2003) Mater Chem Phys 80:169
9. Bouklah M, Benchat N, Hammouti B, Aouniti A, Kertit S (2006) Mater Lett 60:1901
10. Bentiss F, Traisnel M, Lagrene M (2001) J Appl Electrochem 31:41
11. Hammouti B, Aouniti A, Taleb M, Brighli M, Kertit S (1995) Corrosion 51:411
12. Ramesh S, Rajeswari S, Maruthamuthu S (2003) Mater Lett 57:4547
13. Berchmans LJ, Sivan V, Iyer SVK (2006) Mater Chem Phys 98:395
14. Trachli B, Keddam M, Srhiri A, Takenouti H (2002) Corros Sci 44:997
15. El-Rehim SSA, Ibrahim AMM, Khaled KF (1999) J Appl Electrochem 29:593
16. Ateya BG, El-Khair MBA, Abdel-Hamed IA. (1976) Corros Sci 16:169
17. Abboud Y, Abourriche A, Saffaj T, Berrada M, Charrouf M (2006) Appl Surf Sci 252:8178
18. Bentiss F, Gassama F, Barbry D, Gengembre L, Vezin H, Lagrenee M, Traisnel M (2006) Appl Surf Sci 252:2684
19. Quraishi M, Ahmad S, Venkatachari G. (1996) Bull Electrochem 12:109
20. Ferreira ES, Giancomelli C, Giacomelli FC, Spinelli A (2004) Mater Chem Phys 83:129
21. Juttner K (1990) Electrochim Acta 35:1501
22. Fawcett WR, Kovacova Z, Motheo A, Foss C (1992) J Electroanal Chem 326:91
23. Mansfeld F (1981) Corrosion 36:301
24. Macdonald JR (1987) J Electroanal Chem 223:25
25. Mertens SF, Xhoffer C, Decooman BC, Temmerman E (1997) Corros 53:381
26. Srhiri A, Etman M, Dabosi F (1992) Werkst Korros 43:406
27. Popova A, Sokolova E, Raicheva S, Christov M (2003) Corros Sci 45:33
28. Bouklah M, Hammouti B, Lagrenee M, Bentiss F (2006) Corros Sci 48:2831
29. Elayyachy M, El-Idrissi A, Hammouti B (2006) Corros Sci 48:2470
30. Flis J, Zakroczymski T (1996) J Electrochem Soc 143:2458
31. Khamis E, Bellucci F, Latanision RM, El-Ashry ESH (1991) Corrosion 47:677
32. Ateya BG, El-Anadouli BE, El-Nizamy FMA (1984) Corros Sci 24:497